Design of Dual-band Omnidirectional Horizontally Polarized Dipole Antenna Array with Cylindrical Radome Covered

Junyi Xu, *Graduate Student Member, IEEE*, Sirao Wu, *Member, IEEE*, and Qiang Chen, *Senior Member, IEEE*

***Abstract*—A dual-band omnidirectional horizontally polarized base station antenna with concentric cylinder radome at Sub-6 GHz band is proposed. The high frequency band element layers are arranged between the low frequency band element layers. The dielectric dual-band radome replaces several layers of antenna elements. The radome enlarges the effective aperture of array element of each frequency band so that the elements spacing at the same frequency band can be lengthened over 1.3 wavelength. Both in-band and cross-band isolation are improved. Also, apparent grating lobe does not appear even under such large spacing while the omnidirectional property is kept well. The experiment of the antenna element with radome shows the gain enhancement at both frequencies. 3.03 dBi of gain at 4.05 GHz and 2.5 dBi at 5.75 GHz are observed.**

***Index Terms*—Dual-band, Large spacing array antennas, Fewer elements, Grating lobe, Dielectric radome**

I. INTRODUCTION

IN Beyond 5G (B5G) mobile communication systems, omnidirectional antennas are expected to be utilized in centralized radio access networks (C-RAN) [1-8] with low-cost, stable, high-quality, and high-capacity communication compared with beamforming antennas at the Sub-6 GHz band. Generally, vertically polarized antennas are much more easily to obtain the desired omnidirectional property [9-12]. As horizontally polarized (HP) antenna [13-15] may obtain up to 10 dB diversity gain than vertically polarized (VP) antenna in the urban or indoor wireless environment [16], there is a great demand for the dual-band omnidirectional horizontally polarized (DBOHP) base station antenna.

In past decades, there have been several pieces of research on DBOHP antenna for base station or WLAN use. One of the dual-band methods is utilizing broadband array element to enlarge the original bandwidth [17]. The rectangular slots not only work for impedance matching but also further increase the gain bandwidth. The antenna finally works at 2.8-5.13 GHz with the peak gain of 0.6-3.7 dBi. Another major method is realizing the two frequencies with two resonant components. In [18], a loop-based electrically small planar antenna is proposed for Wi-Fi application. The electrically small loop antenna works at 2.4 GHz and the Alford loop antenna works at 5 GHz. The two elements each can only provide 1.28 dBi at 2.4 GHz and 0 dBi at 5 GHz. Furthermore, multi-modes are also used to generate several operating frequencies [19]. The slot antenna only with feeding folded patch can radiate with half-wavelength mode (e.g., 2.4 GHz) and full-wavelength mode (e.g., 5 GHz). Parasitic patches are added to enlarge the impedance bandwidth at 5 GHz. The antenna finally works with gain of 1.6 dBi at 2.45 GHz and 2.3 dBi at 5.5 GHz. All the antennas mentioned above only have low gain so that numerous elements are necessary to observe enough gain for the coverage required by C-RAN. This brings the complex feeding network and the infrastructure shortage. Also, the frequency selection is limited, because the structures used are only valid when the selected frequencies have the integral multiple relationships.

In this paper, a dual-band omnidirectional horizontally polarized base station antenna with concentric cylinder radome at Sub-6 GHz band is proposed. The high frequency band (f_h) element layers are arranged between the low frequency band (f_l) element layers. The dual band dielectric radome has the ability of replacing the antenna elements. What's more, the radome enlarges the effective aperture of array element of each frequency band so that the elements at the same frequency band can be placed with a large spacing. It provides more space for the sharing of infrastructure [20]. Both in-band and cross-band isolation are improved. Also, apparent grating lobe does not appear even under such large spacing while the omnidirectional property is kept well.

II. THEORETICAL ANALYSIS AND DUAL-BAND RADOME DESIGN

Conventionally, a planar superstrate is introduced above a printed circuit antenna to enhance the antenna directivity [21]. In our research, the dual-band cylindrical radome is chosen to enhance the performance of omnidirectional antenna, because of the symmetry compared to prism.

A. Antenna Configuration

In Fig. 1, the configuration of proposed dual-band omnidirectional horizontal polarized (DBOHP) antenna with concentric cylinder radome is described. The layers refer to the f_h are placed between the layers of f_l. The adjacent layers with the same operation frequency band are placed with the spacing

These research results were obtained from the commissioned research (JPJ012368C02201) by National Institute of Information and Communications Technology (NICT), Japan. *Corresponding author: Junyi Xu.*

The authors are with the School of Engineering, Tohoku University, Sendai 980-8579, Japan (e-mail: xu.junyi.p8@dc.tohoku.ac.jp; wu.sirao.s4@dc.tohoku.ac.jp; qiang.chen.a5@tohoku.ac.jp).

of h_{a1} and h_{a2} for f_l and f_h, respectively. The radius of the conducting cylinder is r_0, which mainly influences the roundness of the radiation pattern. The radius of the inner dielectric radome cylinder is r_2, and the radius of the outer radome is r_3. The horizontally polarized (HP) dipole antenna is utilized as the fundamental array element. All the antenna elements are placed averagely on the circumference with the radius of r_1. The dual-band radome is made of the same medium with relative permittivity of ε_r=3. The thickness of the inner radome and outer radome is t_1 and t_2, respectively.

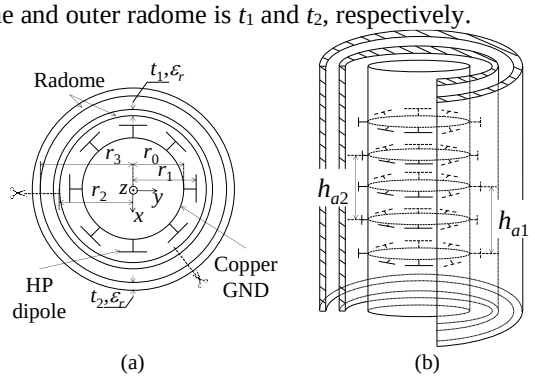

Fig. 1. Proposed antenna array with dual-band radome surrounding. (a) Top view. (b) Structure image.

B. Dual-band Radome Design

In the theory of Fabry-Perot [22] antenna, the resonant condition can be derived as the following equation.

$$\varphi + \pi - \frac{4\pi d}{\lambda} = 2k\pi,\ k = 0,1,2,\ldots \tag{1}$$

where ϕ refers to the phase of the reflection coefficient of the proposed radome and d refers to the distance between radome and ground plane.

When the resonant condition is satisfied, the maximum directivity can be expressed as followed.

$$D_{max} = \frac{1+p}{1-p} \tag{2}$$

where p refers to the magnitude of the reflection coefficient of the proposed radome.

The exact phase curve of the dielectric superstrate can be observed from the calculation of equivalent characteristic impedance. Taking a two-layer case for example, the equivalent model is shown in Fig. 2(a). The results are expressed as in (3) and (4).

$$\begin{cases} \eta_{ef1} = \eta_1 \frac{\eta_0 + j\eta_1 \tan(\beta_1 t_1)}{\eta_1 + j\eta_0 \tan(\beta_1 t_1)} \\ \eta_{ef2} = \eta_0 \frac{\eta_{ef1} + j\eta_0 \tan(\beta_0 t_3)}{\eta_0 + j\eta_{ef1} \tan(\beta_0 t_3)} \\ \eta_{ef3} = \eta_1 \frac{\eta_{ef2} + j\eta_1 \tan(\beta_1 t_2)}{\eta_1 + j\eta_{ef2} \tan(\beta_1 t_2)} \end{cases} \tag{3}$$

$$\Gamma = pe^{j\varphi} = \frac{\eta_{ef3} - \eta_0}{\eta_{ef3} + \eta_0} \tag{4}$$

The intersections of the ideal phase curve in (1) and the exact phase curve ϕ in (4) of the dielectric superstrate are the operation frequency. And the directivity is in direct proportion to the amplitude of the reflection coefficient.

In single frequency single radome case [23], the thickness of radome is set as $\lambda_g/4$. The effect on directivity enhancement is not significant in both frequencies when only one layer is utilized [24]. Therefore, more layers providing effective $\lambda_g/4$ at another frequency should be utilized as the radome such as two layers with air gap.

The design is based on the double-layer structure for 5 GHz with thickness of $\lambda_g/4$ and air gap of $\lambda_0/4$, which originally was used to enhance the gain performance in single frequency case. Choosing d=30 mm as the distance between the ground plane and the dual-band radome, the final parameters are shown in Fig. 2. The determined two frequencies are 4.05 GHz and 5.75 GHz.

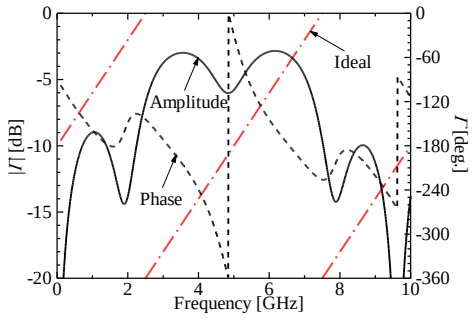

Fig. 2. Magnitude and phase of calculated reflection coefficient. The red dash dot dash line stands for the ideal phase.

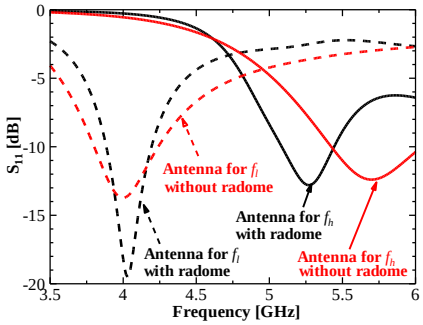

Fig. 3. The reflection coefficient of the antenna with and without cylinder radome.

III. Large Spacing Dual-band Antenna Array

A. Large Spacing Via the Dual-band Radome

To satisfy the roundness of DBOHP antenna, 8 HP dipole elements are utilized in the same layer. And multi-layer structure is used to observe high directivity. The dual-band radome increases the effective aperture of the antenna, which gives the possibility to extend the distance between two adjacent elements when constructing an array.

Fig. 3 shows the reflection coefficient of 8 HP elements omnidirectional antenna with and without radome. It is obvious that the existence does not affect the impedance matching at f_l. But it brings frequency shift at f_h. Therefore, in simulation, directivity is used to evaluate the performance of proposed antenna.

Fig.4(a). Fig.4(b) and (c) show the radiation patterns of the 3-layer DBOHP antenna in the vertical plane at 4.05 GHz and 5.75 GHz, respectively. At 4.05 GHz, the concentric cylindrical radome extends the layer spacing to 1.3 wavelength without creating the apparent grating lobe, while the 7 dBi average directivity in the horizontal plane is kept. Similarly, at 5.75 GHz, the layer spacing is extended to 1.5 wavelength, while keeping same average directivity in the horizontal plane. Therefore, For the dual-band application, the f_h layer can be placed between two adjacent f_l layers with wide spacing compared to the conventional 0.5 wavelength spacing, as shown in Fig.1.

Fig.5 shows the average directivity at f_l and f_h. As the main propose in this article is designing omnidirectional antenna after all, only the average directivity at the frequency with <3 dB roundness is plotted in the figure. At f_l and f_h, around 1 GHz gain bandwidth can be observed. This result means that the antenna is able to maintain the stability and effectiveness of its performance under the frequencies within the 3 dB gain bandwidth.

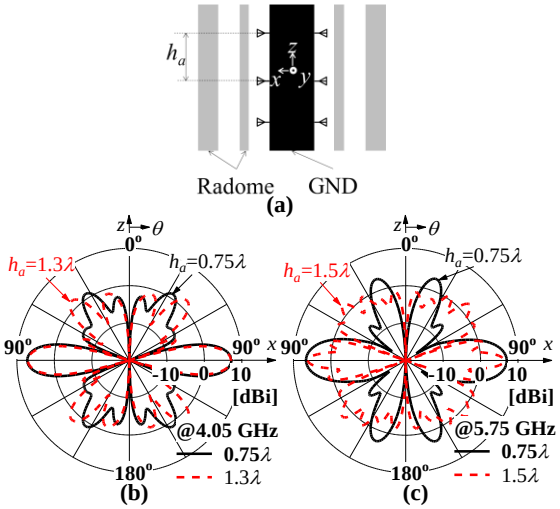

Fig. 4. (a) Structure of 3-layer antenna array with varied spacing. (b) vertical plane radiation pattern at 4.05 GHz. (b) vertical plane radiation pattern at 5.75 GHz.

B. DBOHP Antenna Array

The radiation patterns of the proposed DBOHP antenna with concentric cylindrical radome and conventional DBOHP antenna without radome are presented in Fig. 6. The f_h element layers of 5.75 GHz are placed between the f_l layers of 4.05 GHz with the wide spacing observed from previous results. More antenna layers must be used to guarantee the same directivity level without the radome while keeping the omnidirectional property. It can be observed from Fig. 6(b) and (c) that several antenna layers can be replaced by the dielectric radome, which decreases the complexity and cost of feeding network. The cross-band isolation [25] is 25 dB with radome compared with 20 dB without radome. The in-band isolation [26] also improved after introducing the radome by 8.5 dB and 6.5 dB at f_l and f_h, respectively.

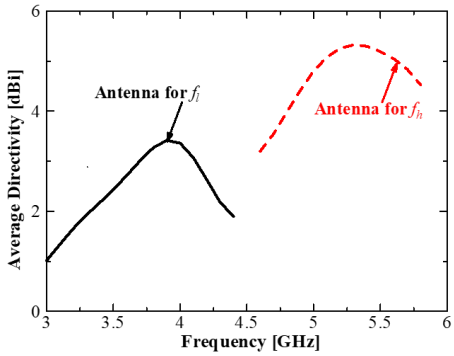

Fig. 5. The average directivity of the antenna with cylinder radome.

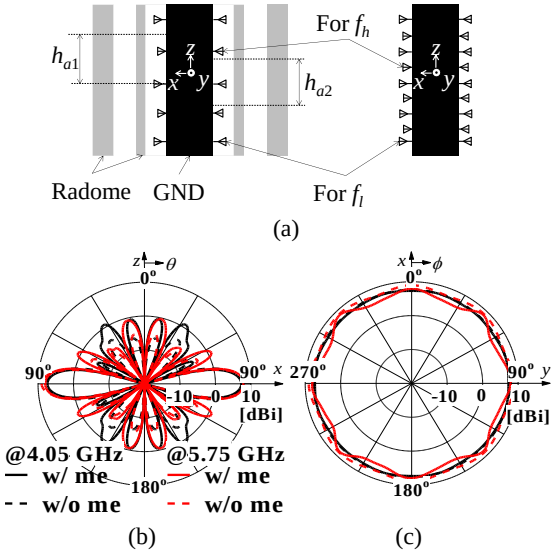

Fig. 6. (a) Structure of antenna with radome and without radome. (b) Radiation pattern in vertical plane. (c) Radiation pattern in horizontal plane.

The roundness can be improved by rotating the adjacent layer with the same frequency [27-29] which is reported as a wideband solution for roundness.

In addition, because only two layers of f_h and three layers of f_l are utilized, further high directivity can be realized by more layers of the HP dipole antenna elements.

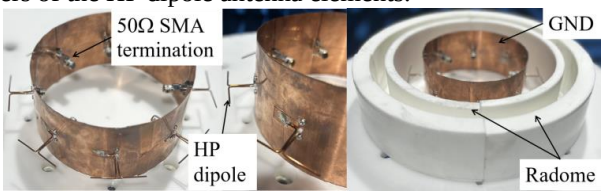

Fig. 7. Fabrication of the proposed antenna.

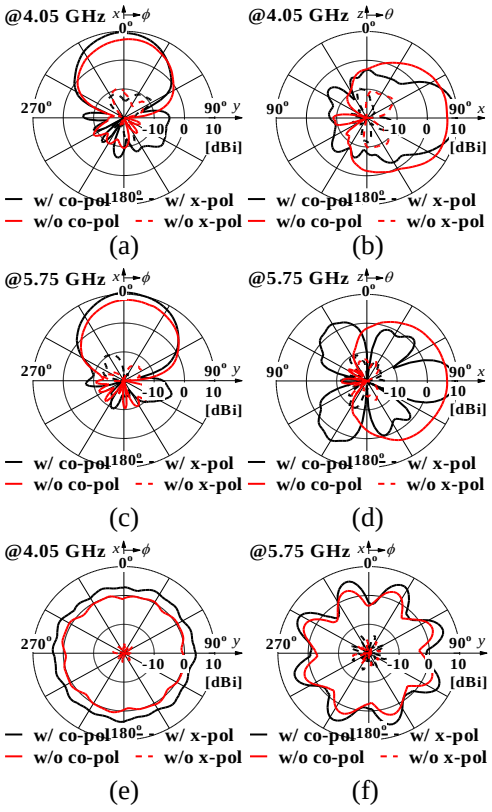

Fig. 8. Experiment results at both frequencies.

IV. Antenna Performance in Experiment

The two 8-element HP cylindrical dipole antenna arrays are fabricated to evaluate the performance of the dual-band radome-covered antenna at 4.05 GHz and 5.75 GHz, respectively. The radome is fabricated by 3D printer using PLA as the material. As shown in Fig. 7, the 8 HP dipole antennas are attached to a cylindrical copper plate. And due to the experiment environment, 7 of them are terminated by 50 Ohm. The last one acts as the feeding point. The radiation pattern with the 8 elements all fed is calculated from the measured 1-element fed pattern.

Because the length of 50 Ohm termination is too long, the radius of copper cylinder in experiment has to be extended. Though it might influence the omnidirectional property, the effect of radome in enlarging the effective aperture of element layer can still be observed.

Fig. 8(a) and (b) presents the experimental radiation patterns of the HP dipole antenna array with and without concentric cylindrical radome in horizontal plane and vertical plane at 4.05 GHz. The peak gain is enlarged after introducing the radome by 2.2 dB. And the beamwidth on the vertical plane is narrowed which meets well with precious simulation result. In Fig. 8(e), the radiation pattern of 8-element fed case is based on the measured 1-element fed case. The average gain is increased to 3.03 dBi (3 dB increment), while the roundness is kept under 3 dB, which means good omnidirectional property.

Also, at 5.75 GHz, as shown in Fig.8(c) and (d), the peak gain increases from 8.07 dBi to 10.59 dBi by introducing the radome. The beamwidth is narrowed in the vertical plane. Still, the radiation pattern of 8-element fed case is based on the measured 1-element fed case and shown in Fig. 8(f). From this figure, the average gain increment on the horizontal plane of 2.5 dBi can be observed. As mentioned previously, the radome affects the impedance matching at fh. Therefore, if the mismatching loss is compensated in practical application, such as using matching circuit, the realized gain might be higher than the gain in Fig.8(f). The worsened roundness for 5.75GHz might be caused by the extension of the radius of the copper cylinder in the experiment, and it can also be improved by the above-mentioned array later rotation.

According to the experiment results, it can also be seen that the proposed antenna in this research can present the good omnidirectional property and high gain requirement.

Table R1 Comparison on previous works and this work

	Freq. Band	Freq [GHz]	G_E[a] [dBi]	G_A[b] [dBi]	Num.[c]	h_a[d] [λ]
[17]	Wide band	2.8-5.13	0.6-3.7	N/A	N/A	N/A
[18]	Dual band	2.4 & 5	1.28 & 0	N/A	N/A	N/A
[19]	Dual band	2.45 & 5.5	1.6 &2.3	N/A	N/A	N/A
[28]	Wide band	1.71–2.69	1.2-2.5	6.65-8.11	6	0.7
This work	Dual band	4.05 & 5.75	3.03 & 2.5	7.8 & 7.27	3 & 2	>1.3

[a]G_E=Gain of Element, [b]G_A=Gain of array, [c]Num.=Element Number, [d]h_a=Array Spacing.

V. Conclusion

A dual-band omnidirectional horizontally polarized base station antenna with concentric cylindrical dielectric radome at Sub-6 GHz band was proposed. The f_h element layers were arranged between the f_l element layers. Several antenna elements were replaced by the dual-band dielectric radome. The radome enlarged the effective aperture of array element of each frequency band so that the elements at the same frequency band could be placed with a large spacing compared with conventional 0.7-0.8 wavelength case. Both in-band and cross-band isolation were improved. Also, apparent grating lobe did not appear even under such large spacing while the omnidirectional property was kept well. The experiment of the antenna element with radome showed the gain enhancement at both frequencies. 3.03 dBi of gain at 4.05 GHz and 2.5 dBi at 5.75 GHz were observed. Although further optimization is required.

Acknowledgment

These research results were obtained from the commissioned research (JPJ012368C02201) by National Institute of Information and Communications Technology (NICT), Japan.

References

[1] O. Woodward and J. Gibson, "The omniguide antenna; An omnidirectional waveguide array for UHF-TV broadcasting," *1958 IRE International Convention Record*, New York, NY, USA, 1955, pp. 37-39.

[2] J. Chu; Physical Limitations of Omni-Directional Antennas. *J. Appl. Phys.* 1 December 1948; 19 (12): 1163–1175.

[3] X. Quan and R. Li, "A broadband dual-polarized omnidirectional antenna for base stations," *IEEE Trans. Antennas Propag.*, vol. 61, no. 2, pp. 943–947, Feb. 2013.

[4] S. Wen, Y. Xu, and Y. Dong, "A low-profile dual-polarized omnidirectional antenna for LTE base station applications," *IEEE Trans. Antennas Propag.*, vol. 69, no. 9, pp. 5974–5979, Sep. 2021.

[5] J. Wang, L. Zhao, Z.-C. Hao, and J.-M. Jin, "A wideband dual-polarized omnidirectional antenna for base station/WLAN," *IEEE Trans. Antennas Propag.*, vol. 66, no. 1, pp. 81–87, Jan. 2018.

[6] C.-C. Lin, L.-C. Kuo, and H.-R. Chuang, "A horizontally polarized omnidirectional printed antenna for WLAN applications," *IEEE Trans. Antennas Propag.*, vol. 54, no. 11, pp. 3551–3556, Nov. 2006.

[7] S. Xia, C. Ge, Q. Chen, and F. Adachi, "A study on user-antenna cluster formation for cluster-wise MU-MIMO," *Proc. 23rd Int. Symp. Wireless Pers. Multimedia Commun.*, 2020, pp. 1–6.

[8] S. Wu, J. Xu and Q. Chen, "High-Gain Omnidirectional Horizontally Polarized Dipole Array for Sub-6 Base Station," *IEEE Antennas Wireless Propag. Lett*, vol. 22, no. 7, pp. 1652-1656, July 2023.

[9] T. J. Judasz and B. B. Balsley, "Improved theoretical and experimental models for the coaxial colinear antenna," *IEEE Trans. Antennas Propag.*, vol. 37, no. 3, pp. 289–296, Mar. 1989.

[10] H. Miyashita, H. Ohmine, K. Nishizawa, S. Makino, and S. Urasaki, "Electromagnetically coupled coaxial dipole array antenna," *IEEE Trans. Antennas Propag.*, vol. 47, no. 11, pp. 1716–1726, Nov. 1999.

[11] K.-L. Wong, F.-R. Hsiao, and T.-W. Chiou, "Omnidirectional planar dipole array antenna," *IEEE Trans. Antennas Propag.*, vol. 52, no. 2, pp. 624–628, Feb. 2004.

[12] K. Wei, Z. Zhang, W. Chen, Z. Feng, and M. F. Iskander, "A triband shunt-fed omnidirectional planar dipole array," *IEEE Antennas Wireless Propag. Lett.*, vol. 9, pp. 850–853, 2010.

[13] Y. Yu, F. Jolani, and Z. Chen, "A wideband omnidirectional horizontally polarized antenna for 4G LTE applications," *IEEE Antennas Wireless Propag. Lett.*, vol. 12, pp. 686–689, 2013.

[14] C. H. Ahn, S. W. Oh, and K. Chang, "A dual-frequency omnidirectional antenna for polarization diversity of MIMO and wireless communication applications," *IEEE Antennas Wireless Propag. Lett.*, vol. 8, pp. 966–970, 2009.

[15] H.-R. Chuang and L.-C. Kuo, "3-D FDTD design analysis of a 2.4- GHz polarization-diversity printed dipole antenna with integrated balun and polarization-switching circuit for WLAN and wireless communication applications," *IEEE Trans. Microw. Theory Techn.*, vol. 51, no. 2, pp. 374–381, Feb. 2003.

[16] D. Chizhik, J. Ling and R. A. Valenzuela, "The effect of electric field polarization on indoor propagation," *ICUPC '98.* (Cat. No.98TH8384), Florence, Italy, 1998, pp. 459-462 vol.1.

[17] Wu, Shihao, and Feng Shang. "5G Indoor Base Station Application: Low Profile Broadband Horizontally Polarized Omnidirectional Antenna." *Prog. Electromagn. Res. C* 133 (2023): 15-25.

[18] P. F. Hu, K. W. Leung, Y. M. Pan and S. Y. Zheng, "Electrically Small, Planar, Horizontally Polarized Dual-Band Omnidirectional Antenna and Its Application in a MIMO System," *IEEE Trans. Antennas Propag.*, vol. 69, no. 9, pp. 5345-5355, Sept. 2021.

[19] J. Guo, H. Bai, A. Feng, Y. Liu, Y. Huang and X. Zhang, "A Compact Dual-Band Slot Antenna With Horizontally Polarized Omnidirectional Radiation," *IEEE Antennas Wireless Propag. Lett.*, vol. 20, no. 7, pp. 1234-1238, July 2021.

[20] K. Samdanis, X. Costa-Perez and V. Sciancalepore, "From network sharing to multi-tenancy: The 5G network slice broker," *IEEE Commun Mag.*, vol. 54, no. 7, pp. 32-39, July 2016.

[21] D. Jackson and N. Alexopoulos, "Gain enhancement methods for printed circuit antennas," *IEEE Trans. Antennas Propag.*, vol. 33, no. 9, pp. 976-987, September 1985.

[22] G. V. Trentini, "Partially reflecting sheet arrays," *IRE Trans. Antennas Propag.*, vol. 4, no. 4, pp. 666-671, October 1956.

[23] J. Xu, S. Wu and Q. Chen, "Sub-6 GHz Band Omnidirectional Horizontally Polarized Large Spacing Array Antenna With Dielectric Radome for Base Station," *IEEE Access*, vol. 11, pp. 139915-139923, 2023.

[24] Junyi, Xu, Sirao Wu, and Qiang Chen. "Dual-band antennas with high-gain and omni-directional radiation pattern enhanced by single-layer radome." *IEICE Commun. Express.* 12.8 (2023): 409-414.

[25] . Zhu, Y. Chen and S. Yang, "Cross-Band Mutual Coupling Reduction in Dual-Band Base-Station Antennas With a Novel Grid Frequency Selective Surface," *IEEE Trans. Antennas Propag.*, vol. 69, no. 12, pp. 8991-8996, Dec. 2021.

[26] Y. Da, X. Chen and A. A. Kishk, "In-Band Mutual Coupling Suppression in Dual-Band Shared-Aperture Base Station Arrays Using Dielectric Block Loading," *IEEE Trans. Antennas Propag.*, vol. 70, no. 10, pp. 9270-9281, Oct. 2022.

[27] M. S. Siukola, "The Traveling-Wave VHF Television Transmitting Antenna," *IRE Trans. Broadcast Telev. Receiv.*, vol. BTR-3, no. 2, pp. 49-58, Oct. 1957.

[28] L. H. Ye, Y. Zhang, X. Y. Zhang and Q. Xue, "Broadband Horizontally Polarized Omnidirectional Antenna Array for Base-Station Applications," *IEEE Trans. Antennas Propag.*, vol. 67, no. 4, pp. 2792-2797, April 2019.

[29] H. R. D. Filgueiras, I. F. da Costa, A. Cerqueira S., J. R. Kelly and P. Xiao, "A Novel Approach for Designing Omnidirectional Slotted-Waveguide Antenna Arrays," *2018 International Conference on Electromagnetics in Advanced Applications (ICEAA)*, Cartagena, Colombia, 2018, pp. 64-67,.